

## Cavitation Bubbles in a Starting Submerged Water Jet

K.Nakano, M.Hayakawa, S.Fujikawa and T.Yano

*Graduate School of Engineering, Hokkaido University, Sapporo, Japan*

### Abstract

The behavior of cavitation bubbles in a starting submerged water jet discharging from a circular nozzle is studied by a simple photography technique in a moderately low range of jet exit velocity. A number of small spherical bubbles are initially generated in a starting vortex formed at the jet tip and often connected circumferentially with each other in the form similar to a vortex ring. Nearly axisymmetric lumps of disconnected bubbles are also observed frequently. By analyzing photographic data acquired from the side and end view pictures of the ring-like bubbles, their average properties, such as trajectory, geometry and size, are evaluated.

### 1. Introduction

It is well known that the cavitation inception occurs when cavitation nuclei in a liquid are exposed to a sufficiently low pressure, comparable with the vapor pressure of the liquid, to cause their unstable and explosive growth (Arndt 1981; Brennen 1995).

In submerged water jets where the mean static pressure is generally much higher than vapor pressure, the onset of cavitation is believed to take place in low pressure regions produced by vortical structures. Observations by Ooi(1985) and Gopalan et al.(1999) show that the cavitation inception in initially laminar jets does not occur in the cores of rolled-up vortices but in the cores of secondary vortices which are formed randomly. This suggests that the investigations of the generation process of bubbles are quite difficult in turbulent regions in jets. One of the approaches to circumvent the difficulty would be to deal with cavitating jet flows, where well-organized vortices are formed either periodically or reproducibly, such as in a self-excited jet (Chahine & Genoux 1983).

In the present work, we employ an impulsively-started jet, where a starting vortex of the jet should produce nearly axisymmetric low pressure. This low pressure may lead to the formation of ring-like cavitation bubbles in the near field of the jet. We shall study the behavior of such ring-like cavities.

### 2. Experimental setup and conditions

The experimental apparatus consists of a closed water reservoir connected to an air compressor, a water reservoir opened to the atmosphere, and a 15mm-diameter circular pipe connecting the two reservoirs, as shown in Fig.1. Water flow is operated by an electromagnetic valve and discharged into a still water from an orifice-type nozzle with the exit diameter of

5mm. A piezoelectric pressure transducer with the resonance frequency of about 300kHz is mounted in the pipe at 65mm upstream the nozzle exit.

The output signal of the transducer is used to measure the transient pressure change of water in the pipe, as well as to detect the onset of flow and to trigger a light source for photography. The light source is a flash light with the nominal lightening duration of 0.0002 ms which is short enough for individual cavitation bubbles to be captured as still images in pictures under the present test conditions. Flow observations are made by two cameras; one is located just downstream and above the nozzle exit, and the other is outside the open reservoir and facing to the nozzle exit section.

Experiments were performed for the gauge pressure level,  $p_g$ , of the closed water reservoir in the range 0.3 - 0.5MPa, and the cross-sectional mean velocity,  $U_j$ , at the nozzle exit in the range 15.3 - 19.5m/s. The corresponding Reynolds numbers based on  $U_j$  and orifice diameter  $D(=5mm)$  are  $(7.5 - 10) \times 10^5$ . Tap water was used without any treatment for degassing, so that the dissolved air content would be in a nearly saturated condition. Water temperature was kept  $20 \pm 3$  C throughout the experiments.

Figure 2 shows an example of the pressure transducer signal, where  $p^*$  indicates the difference in water pressure across the nozzle, and the origin in time  $t$  is arbitrary. The mechanism of the electromagnetic valve used is such that as electric current is supplied, a subsidiary valve(called "pilot valve") opens first and a small amount of water discharges, and thereafter a main valve starts to open. Owing to this mechanism,  $p^*$  shows first a bump and then a sharp rise, followed by a gradual increase to the maximum. Because the bump was found to appear reproducibly prior to the onset of the main flow, we used it as the trigger signal of flashing the light and also as the temporal origin in the results to be presented.

### 3. Results

We visualized first starting vortices using dye-marked water. Soon after the flow was initiated, a mushroom-shaped concentration of dye was observed at the jet tip. When  $p_g > 0.4MPa$ , the mush-room-shaped structure was followed by another large concentration of dye. These concentrations are both associated with starting vortices; that is, the leading one is due to the pilot valve opening and the second one to the main valve opening.

Similar observations, repeatedly made by reducing the amount of dye, showed that spherical bubbles appear mostly in the leading and the second dye-concentrated regions, and tend to be aligned in the azimuthal direction to take a form similar to a ring. This suggests that the cavitation inception does occur inside the starting vortices. In later stages of jet development, smaller bubbles were found to be formed behind the starting vortices; some were in groups and the others were randomly distributed in the jet shear layer. In what follows, results obtained at  $p_g = 0.5MPa$  will be presented, with primarily focusing on the behavior of ring-like lumps of bubbles.

Some side-view pictures taken at different stages of jet development are shown in Figs. 3(a-d). We have confirmed from many close-up pictures that most of ring-like lumps of bubbles consist of a number of small and nearly spherical bubbles, and the shapes of lumps resemble rosaries or circular chains of beads, rather than azimuthally uniform rings. Ring-

like lumps of disconnected bubbles were also observed frequently (see, for example, Fig.3c). Bubbles at the jet tip were even smaller and often isolated due to the comparatively weak circulation of the leading vortex caused by the pilot-valve opening. For convenience of description, the ring-like lump of bubbles, including disconnected ones, will be hereafter referred to as "bubble ring".

Figures 4 shows the streamwise position of bubble rings as a function of time, where the leading and the second bubble rings are shown by triangles and circles, respectively. The leading and the second bubble rings move downstream with distinctly different velocities; the former travels slower at roughly  $4m/s$  and the latter at  $10m/s$  in  $x/D < 8$ . When two bubble rings are successively formed, the second bubble ring catches up and interacts with the leading one at around  $x/D = 6$  (see, for example, Fig.3d).

Observations of end-view pictures showed that almost all the bubble rings seldom maintain the axisymmetric shape as convected downstream, and often undergo a wavy deformation, probably reflecting the occurrence of the azimuthal instability of a vortex ring (Widnall & Sullivan 1973). The bubble rings were found to persist downstream up to  $x/D = 15 - 20$ , but it was not clear to what extent they could survive, because of the increasing distortion and diffusion of bubble rings further downstream.

Figures 5(a,b) show the streamwise variations of the average diameter  $D_r$  and thickness  $d_r$  of bubble rings, which were evaluated from the side- and/or end-view pictures. The diameter  $D_r$ , which is initially close to the orifice diameter, increases with  $x$  in accordance with the vortex ring growth. The thickness of bubble rings appears to reach its maximum at  $x/D = 3-4$ , followed by a gradual decrease with increasing  $x$ . From  $D_r$  and  $d_r$ , we calculated the approximate volume  $V_r$  of bubble ring, with assuming its geometry to be a torus. The result is shown in Fig.6, where  $V_r$  is represented in a logarithmic scale. The volume exhibits a rapid increase up to about  $x/D = 3$ , beyond which it does not increase any further, in contrast to the continuous increase of the bubble ring diameter.

Figure 7 shows the average diameter,  $d_i$ , of individual bubbles forming a bubble ring. The typical size of bubbles contained in the bubble ring exhibits an abrupt increase soon after its formation, followed by a gradual decrease.

These results indicate that outside the formation region, the evolution of bubble rings is not much affected by the dissolved air in water surrounding the jet flow. In particular, the approximately constant values of  $V_r$  and  $d_i$  in  $x/D > 5$  suggest that no significant air entrainment occurs beyond the jet potential core during the evolution of bubble rings.

#### 4. Conclusions

Cavitation bubbles in a starting water jet were studied in a moderately low range of jet exit speed. The reproducible nature of the starting jet helped us to observe the behavior of bubbles by a simple photography technique. The main results are summarized as follows.

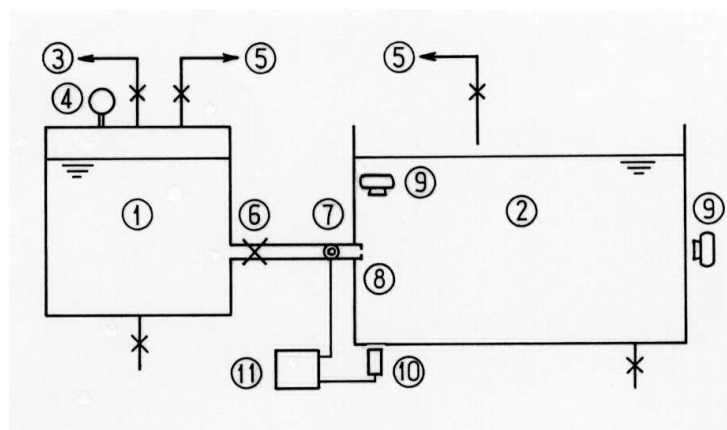
- (1) In early stages of jet development, cavitation bubbles are mostly generated inside the starting vortices and connected with each other in the form of a ring.

- (2) Once formed, the bubble rings travel downstream with the starting vortices and often survive beyond 20 times the nozzle diameter.
- (3) The average size of the individual bubbles forming the bubble rings quickly increases in the vicinity of nozzle and then gradually decreases as they travel downstream.
- (4) In later stages of jet development, isolated bubbles are formed behind the starting vortices; some are in groups and others are randomly distributed in the jet shear layer.

The authors would like to thank Mr. Yutaka Nozaki for his help in constructing experimental facilities and devices.

## References

- Arndt, R.E.A 1981 Cavitation in fluid machinery and hydraulic structures. *Ann.Rev. Fluid Mech.* **13**, 273-328.
- Brennen, C.E. 1995 *Cavitation and Bubble Dynamics*, Oxford University Press.
- Chahine, G.L and Genoux, Ph.F. 1983 Collapse of a cavitating vortex ring. *J.Fluids Engg.* **105**, 400-405.
- Gopalan, S., Katz, J. and Knio, O. 1994 The flow structure in the near field of jets and its effect on cavitation inception. *J.Fluid Mech.* **398**, 1-43.
- Ooi, K.K. 1985 Scale effects on cavitation inception in submerged water jets: a new look. *J.Fluid Mech.* **151**, 367-390.
- Widnall, S.E. and Sullivan, J.P. 1973 On the stability of vortex rings. *Rroc.Roy.Soc. Lond. A* **33**, 335-353.



- (1) Closed water tank (2) Water reservoir (3) Air compressor (4) Pressure gauge  
 (5) Water supply (6) Electromagnetic valve (7) Pressure sensor/ transducer  
 (8) Orifice-type nozzle (9) Camera (10) Flash light (11) Pulse circuit

Figure 1. Schematic of experimental setup.

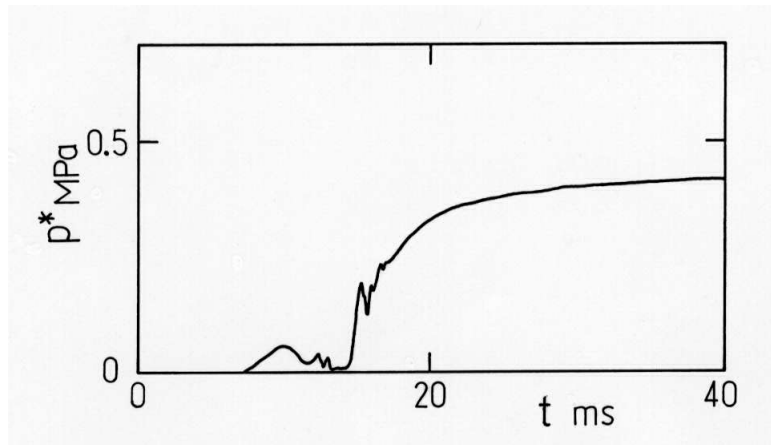


Figure 2. An example of pressure transducer signal;  $p_g = 0.5 \text{ MPa}$ .

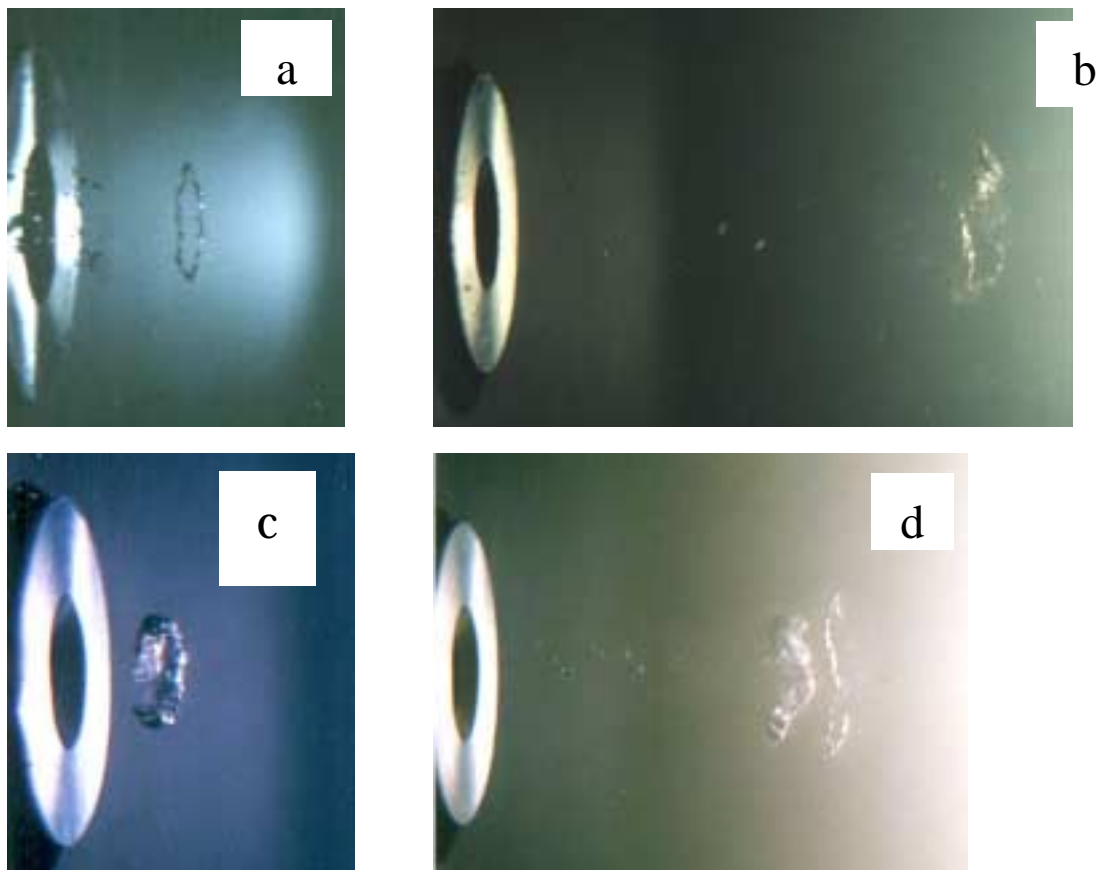


Figure 3. Four examples showing bubble rings. Flow is from left to right.

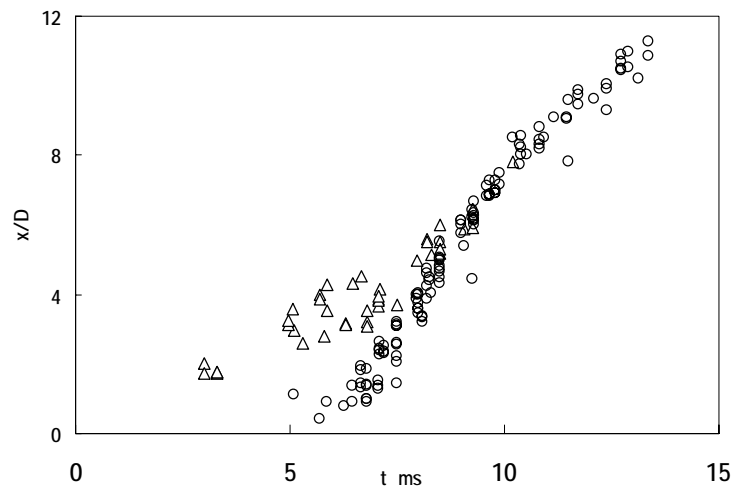


Figure 4. Streamwise position of bubble rings as a function of time.

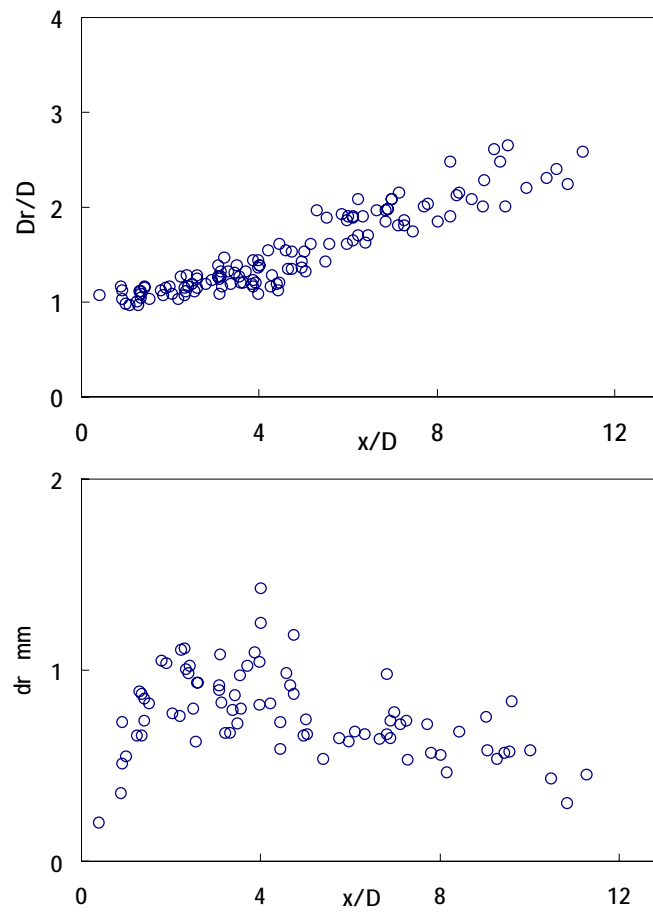


Figure 5. Diameter and thickness of bubble rings; (a) diameter, (b) thickness.

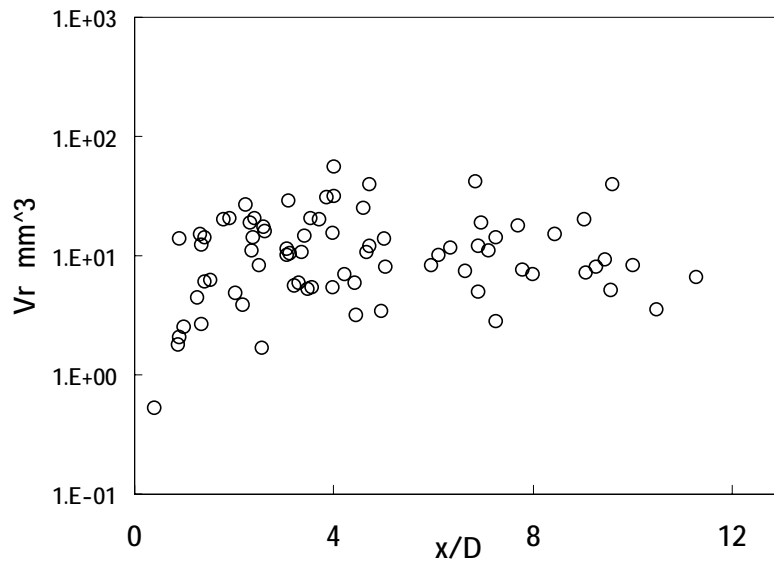


Figure 6. Approximate volume of bubble rings.

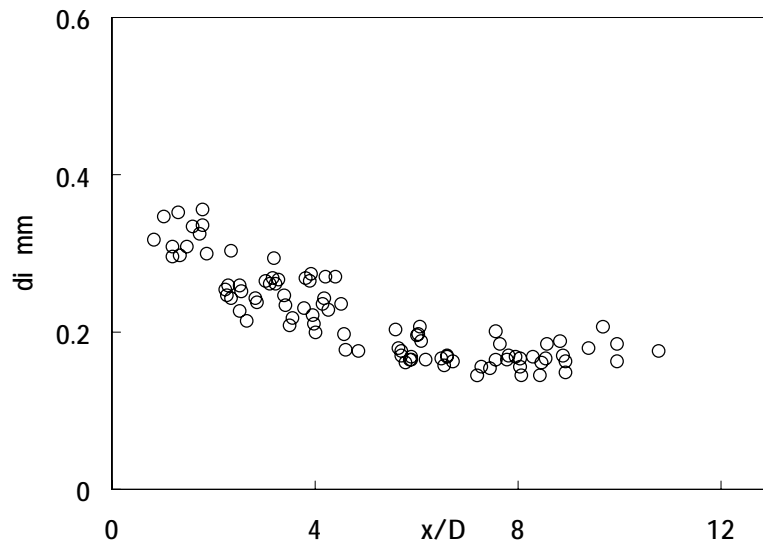


Figure 7. Average diameter of individual bubbles in bubble rings.